A Trapped Photoelectron Instability in Electron and Positron Storage Rings

T. Holmquist and J. T. Rogers
Laboratory of Nuclear Studies, Cornell University, Ithaca, New York 14853
(Received 1 May 1997)

An anomalous growth of the horizontal coupled bunch modes of the bunched beam is observed in the Cornell Electron Storage Ring. In contrast with instabilities caused by electromagnetic wake fields, the growth rate is a highly nonlinear function of the bunch charge. We show that this effect is due to photoelectrons produced by synchrotron radiation which are trapped in the beam chamber by the bending magnet field and a quadrupole electrostatic field. We have developed a numerical simulation and an analytical model of this process. [S0031-9007(97)04354-8]

PACS numbers: 29.27.Bd, 29.20.Dh

In storage rings, electromagnetic wake fields produced by the passage of the beam through the vacuum chamber couple the motion of different bunches. In general, the perturbed oscillation frequencies have an imaginary part, so that some of the coupled bunch modes have a positive growth rate, which is proportional to the beam current.

In contrast to this linear model of beam instability, an anomalous transverse coupled bunch instability ("anomalous antidamping"), in which the growth rate is a nonlinear function of beam current, is observed in the Cornell Electron Storage Ring (CESR) [1]. The absolute value of the growth rate is largest at the intermediate currents encountered during injection, and becomes dramatically smaller at higher currents. The instability is predominantly horizontal. Coupled bunch modes at positive frequencies are damped; those at negative frequencies tend to grow. The absolute value of the growth rate decreases monotonically with mode frequency. If the beam consists of trains of bunches spaced by 28 ns or less, the bunches within a train move coherently. The growth rate is similar for positrons and electrons except for minor differences which may be due to Landau damping from ion capture by the electron beam [2]. Measurements shown here were performed with positrons so that the growth rate is independent of residual gas pressure. Beams in collision are stable because of the Landau damping provided by the nonlinear beam-beam force.

The anomalous instability is present only when the distributed ion pumps (DIPs) are powered [3]. It disappears immediately when the DIPs are turned off. The growth rate is proportional to the number of DIPs powered and to the DIP anode voltage [4]. CESR contains DIPs in all bending magnets. Pumping slots allow the electrostatic field from the DIP anode to leak into the beam chamber. The calculated potential [5,6] is shown in Fig. 1. Some CESR DIPs have additional shields which suppress the leakage field. These pumps have no effect on the beam.

We hypothesize [7] that slow electrons trapped in the beam chamber are responsible for the anomalous instability. These electrons are produced through photoemission by synchrotron radiation striking the beam chamber walls and are trapped in the combined dipole magnetic field and quadrupole electrostatic leakage field from the distributed ion pumps. Repeated passages of the beam eject them. In this way the position of the beam modulates the trapped charge density, which in turn exerts a time-dependent force on the beam. Photoelectrons are confined horizontally by the 0.2 T dipole magnet field. The leakage field from the DIP slots confines the electrons vertically, much like a Penning trap. The horizontal component of the DIP leakage field causes an $\mathbf{E} \times \mathbf{B}$ drift down the length of the magnet, with a velocity of the order of 10^3 m/s. Electrons are removed by interactions with the beam on a time scale of tens of microseconds [6], so electron loss by drift is negligible. The cyclotron motion of the electrons at 5.6 GHz is unimportant at the frequencies of the coupled bunch modes. The vertical motion of the electrons, with frequencies of several MHz, dominates the dynamics.

A numerical model was produced to calculate the coupled bunch growth rate [6]. In this model, electron macroparticles move under the influence of the electric field of the DIPs, bunched beam, and their own space charge. Velocities, positions, and fields are updated each time step of 0.5 ns. Secondary emission is modeled by

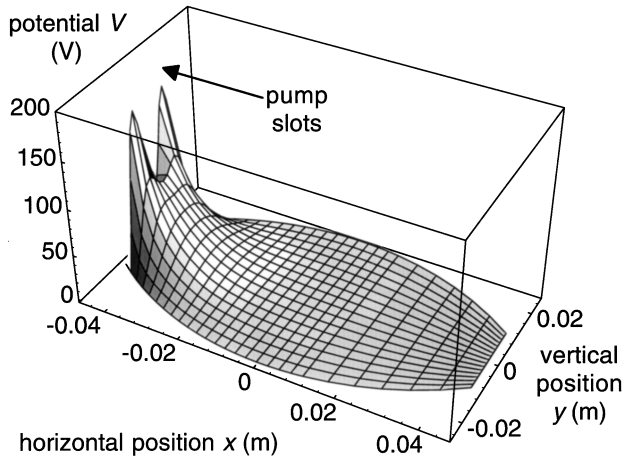

FIG. 1. Electrostatic potential in the CESR beam chamber due to the distributed ion pump.

 0031-9007/97/79(17)/3186(4)$10.00

injecting one or more macroparticles, depending on the secondary emission yield at the incident electron energy. During the beam passage, smaller time steps are used in which several photoelectron macroparticles are injected with a uniform velocity distribution. We have used a value of the photocurrent per unit beam current per unit length for the aluminum chamber which nearly reproduces the measured current dependence of the instability growth rate. This value is consistent with an extrapolation of the photoemission rate measured at DCI [8] to CESR parameters. The reflectivity of the vacuum chamber is unknown, but for any reflectivity between 0 and 1 the illumination of the top and bottom walls of the vacuum chamber is nearly uniform [6]. Photoelectrons emitted by the vertical side wall of the chamber are immediately reabsorbed due to their cyclotron motion and have no effect. The simulation physical parameters are summarized in Table I.

Figure 2 shows the calculated electron charge density 10 ns after the passage of a leading bunch of $3.60 \times 10^{10} e^+$ in a pattern of nine trains of two bunches separated by 28 ns. The pumping slots are to the left. The total charge emitted from the top and bottom walls is 0.161 nC/m. New photoelectrons are evident as bands at the top and bottom of the chamber. Photoelectrons which have been slowed by the space charge of the leading photoelectrons may be trapped on low-amplitude trajectories. The passage of subsequent bunches eventually ejects these trapped electrons. A negligible fraction of electrons is due to secondary emission. An avalanche may be created when electrons close to a bunch are accelerated to an energy for which the secondary emission yield exceeds unity [9]. In CESR, most electrons have left the vicinity of the beam by the next train passage, and no avalanche occurs.

The growth rate of the lowest frequency coupled bunch mode was calculated from the force on the horizontally oscillating beam and is shown for the 9×2 bunch pattern in Fig. 3. Error bars on the simulation points show the effect of the limited number of macroparticles. The simulation shows chaotic behavior which leads to a large scatter in the calculated growth rates. Chaotic dynamics may be expected because the system has three dynamical variables (beam oscillation amplitude, phase, and electron density) and a nonlinearity (electron density vs oscillation amplitude). The observed instability appears to be chaotic as well. The beam oscillation is self-limiting, but its amplitude fluctuates rapidly and unpredictably.

TABLE I. Simulation parameters for CESR.

Constant	Value	Units
Photocurrent/beam current/length	-0.028	m^{-1}
Maximum photoelectron velocity	8×10^5	m/s
Maximum secondary emission yield (SEY)	2.5	
Primary electron energy for maximum SEY	390	eV
Horizontal tune	10.5	
Beam energy	5.3	GeV
Storage ring circumference	768	m
Total length of DIPs	408	m

We have also produced an approximate analytical model of photoelectron trapping which predicts the scaling of the growth rate with frequency and with current. The time-varying force on the beam occurs because the strength of the repeated small kicks which remove the trapped electrons depends on the beam position. Because the electrons move in a nonlinear potential, these kicks occur at nearly random oscillation phases, and the electron motion resembles diffusion. We model this diffusion with a Fokker-Planck equation for the phase-space charge density $W(y, \dot{y}, t)$:

$$\frac{\partial W}{\partial t} + \dot{y}\frac{\partial W}{\partial y} + \frac{1}{m}[F_{\rm ext}(y) - eE_{\rm sc}(y)]\frac{\partial W}{\partial \dot{y}} = \frac{\partial^2}{\partial \dot{y}^2}[D(t)W] + S(y, \dot{y}), \quad (1)$$

where y is the vertical coordinate, $F_{\rm ext}(y)$ is the force on the electrons from the DIP field, $E_{\rm sc}(y)$ is the space charge electric field, $D(t)$ is the diffusion coefficient, and $S(y, \dot{y})$ represents the rate at which new photoelectron phase-space charge density is added. We have reduced the problem to a single spatial dimension by assuming that there is no variation of the forces or the diffusion constant in the region of trapped electrons, because the electrons are confined to a small band within the region between the beam and the DIP slots, as demonstrated by the simulation.

The diffusion coefficient depends on an effective distance $r(t)$ from the beam to the band of photoelectrons. For small oscillations of the beam with frequency Ω,

$$D(t) = \frac{[\Delta \dot{y}(t)]^2}{4\Delta t} \approx D_0(1 - \delta e^{i\Omega t}), \quad (2)$$

where $\Delta \dot{y}$ is the kick provided by the beam passage at intervals of Δt, $D_0 \approx (r_e^2 q_b^2 Mc^2 / r_0^2 e^2 T_0)$, r_0 is the mean distance from the beam to the trapped electrons, δ is the amplitude of the horizontal motion of the beam in units of r_0, r_e is the classical electron radius, q_b is the

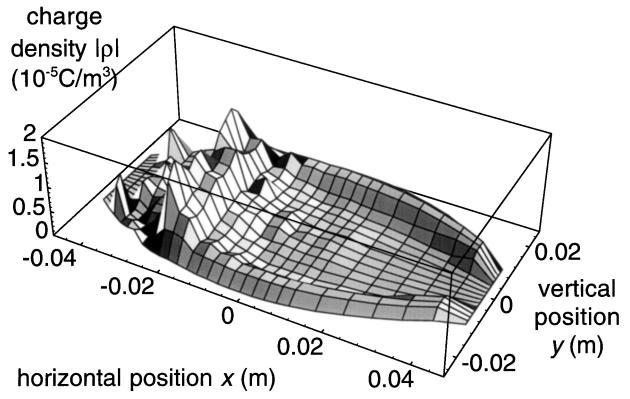

FIG. 2. Calculated charge density in the beam chamber 10 ns after the passage of a bunch.

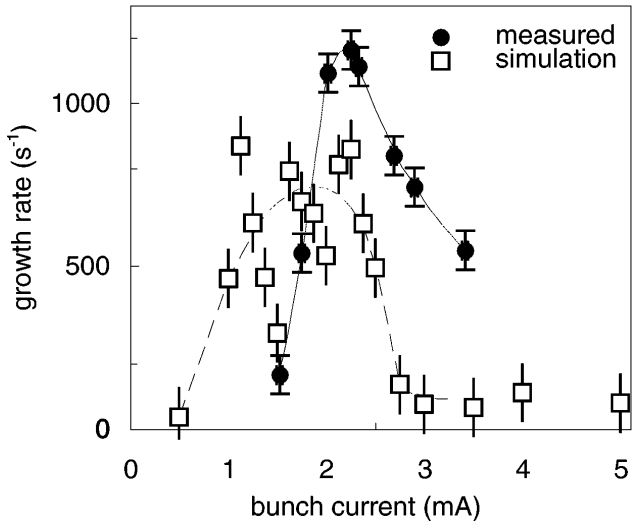

FIG. 3. Horizontal betatron growth rates for the lowest frequency mode, measured in CESR and calculated by the simulation program. The curves are meant only to guide the eye.

bunch charge, M is the number of bunches, and T_0 is the revolution period.

The vertical oscillation period of the trapped electrons is much shorter than the characteristic time for electrons to diffuse out to the chamber wall, so the phase space distribution is approximately symmetric with respect to the phase of the oscillation:

$$W(y, \dot{y}, t) = W(Y, t), \tag{3}$$

$$Y^2 = y^2 + \left(\frac{\dot{y}}{\omega}\right)^2, \tag{4}$$

where ω is the electron oscillation frequency:

$$\omega^2 = -\frac{1}{m}\frac{\partial}{\partial y}[F_{\text{ext}}(y) - eE_{\text{sc}}(y)]. \tag{5}$$

In terms of the new variable Y, the Fokker-Planck equation (1) becomes

$$\frac{\partial W}{\partial t} = \frac{D(t)}{2\omega^2(t)}\frac{\partial^2 W}{\partial Y^2} + S(Y). \tag{6}$$

We must solve this equation for an appropriate choice of $S(Y)$ with the boundary condition $W(Y \geq y_{\text{wall}}, t) = 0$ representing absorbing chamber walls. We can find the solution in two pieces:

$$W(Y, t) = W_0(Y) + w(Y, t), \tag{7}$$

where $W_0(Y)$ is the static solution for $D(t) = D_0$, and $w(Y, t)$ is a time-dependent perturbation. For $S(Y) \propto W_0(Y)$ we have the static solution

$$W_0(Y) = \frac{2\dot{\sigma}_{\text{pe}}\omega_0^2}{(1 - 2/\pi)\pi^2 D_0}\cos\left(\frac{\pi Y}{2y_{\text{wall}}}\right), \tag{8}$$

where $\dot{\sigma}_{\text{pe}}$ is the average photocurrent density. Substituting Eq. (7) and the solution (8) for W_0 into Eq. (6) we obtain the equation for $w(Y, t)$, which, for small oscillations of the beam, has the solution

$$w(Y, 0) = (1 - 2/\pi)^{-1}\cos\left(\frac{\pi Y}{2y_{\text{wall}}}\right) \times \left[\frac{1}{\omega_{\text{ext}}^2}(Aq_b - B)\left(1 + \frac{B}{Aq_b}\right) + 4i\frac{\Omega T_0}{\varepsilon M q_b}y_{\text{wall}}^2\right]^{-1}\delta, \tag{9}$$

where we have defined constants $A = (2\pi c r_e/r_0 e)^2/(8\varepsilon)$, $B = (8\pi r_e y_{\text{wall}} c^2/e)$, $\omega_{\text{ext}}^2 = -(1/m)dF_{\text{ext}}/dx$, and $\varepsilon = (\dot{\sigma}_{\text{pe}} T_0)/(M q_b)$.

The linear charge density from the trapped charge in a band of horizontal width l generates a force on the beam particles from which the impedance can be calculated:

$$Z_1^{\perp}(\Omega) \approx -i\frac{2Lly_{\text{wall}}^2}{\pi I r_0^2 \epsilon_0} \times \left[\frac{1}{\omega_{\text{ext}}^2}(Aq_b - B)\left(1 + \frac{B}{Aq_b}\right) + 4i\frac{\Omega T_0}{\varepsilon M q_b}y_{\text{wall}}^2\right]^{-1}. \tag{10}$$

Here L is the portion of the ring circumference containing DIPs. This is not an impedance in the usual sense because it is current dependent. Note that its real part decreases monotonically with frequency.

We evaluate the growth rate by a summation of the impedance over the distribution of beam frequencies [10]. Several constants can be only roughly estimated, particularly the area photoemission efficiency ε. The chamber reflectivity, which is unknown, is included in ε. The constants r_0, l, and ω_{ext} are estimated from the chamber geometry. Each of these has been chosen to fit the experimental observations. Model constants are summarized in Table II.

The calculated growth rate is shown in Fig. 4. The same model constants are used to fit three bunch data from 1985 [1] and 9×2 bunch data from 1995 [4]. For trains of bunches spaced much more closely than one photoelectron oscillation period $2\pi/\omega$, as in CESR, the effect of the bunch passages within a train is coherent, so the total train charge is substituted for q_b to evaluate

TABLE II. Constants for the CESR photoelectron model.

Constant	Symbol	Value	Units
Area photoemission efficiency	ε	-1.3	m^{-1}
Effective beam-charge distance	r_0	35	mm
Width of trapped charge band	l	10	mm
Chamber half-height	y_{wall}	25	mm
Total length of DIPs	L	408	m
External field constant	ω_{ext}	1.2×10^8	s^{-1}
Horizontal betatron frequency	ω_β	2.582×10^7	s^{-1}

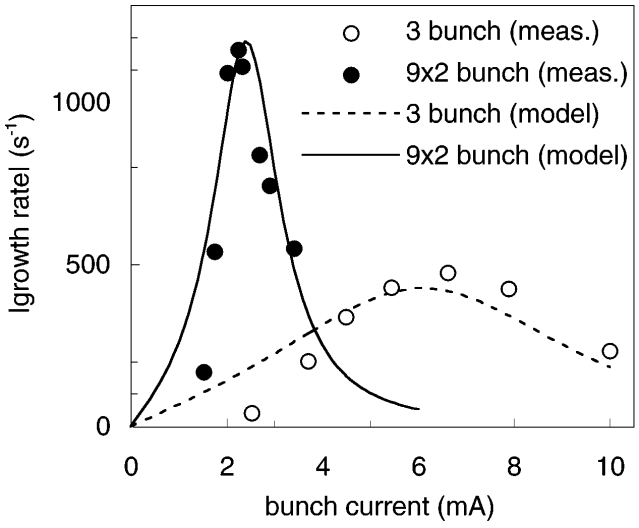

FIG. 4. Horizontal betatron growth rates for the lowest frequency mode, measured in CESR (points) and calculated by the photoelectron model (curves).

the growth rate. The problem has been linearized, so the solution is not chaotic.

An instability caused by the interaction of *free* electrons with a positively charged beam ("electron cloud instability") has been studied theoretically [9,11] and may have been observed in the Photon Factory [12] and the Beijing Electron-Positron Collider (BEPC) [13]. Unlike the trapped electron instability, this instability does not require an external trapping field (e.g., combined quadrupole electric and dipole magnetic fields, or a nonuniform magnetic field). It may occur in the presence or absence of a dipole magnetic field. Unlike the trapped electron instability, the free electron instability occurs only for positively charged beams, because electrons are repelled from a negative beam. The effective wake from the free electron cloud persists only during the transit time of slow electrons across the chamber. In contrast, the wake from the trapped photoelectrons is very long range, because the charge density relaxes back to its equilibrium value several microseconds after being changed by a bunch passage. For the trapped electron wake, the absolute value of the growth rate decreases monotonically with coupled bunch mode frequency. This is not true of the shorter-range free electron wake.

The trapped photoelectron instability occurs for electron or positron beams in the presence of an external trapping field when the transit time for slow electrons across the chamber (less than 100 ns for 1 eV electrons) is less than the bunch spacing. Our simulation shows that the electron density in the chamber is determined by the trapping field for bunch spacing greater than 100 ns, but is independent of the trapping field for bunch spacing less than 10 ns. For these closely spaced bunches, the density is dominated by electrons in their first transit across the chamber, and the instability is of the free electron cloud type. The trapping field has a significant effect in a transition region between 10 and 100 ns.

The trapped photoelectron instability is the dominant transverse instability in CESR, and stable operation of the storage ring requires active feedback. Several e^+e^- colliders and second-generation synchrotron light sources have similar vacuum chamber geometries and the trapped photoelectron impedance should be observable in these as well. We have reduced the instability growth rate in CESR to 18% of its original value by reducing the DIP anode voltage to 25% of the original voltage.

The authors thank E. Chojnacki, K. Ohmi, S. Heifets, J. Byrd, M. Furman, and the members of the CESR Operations Group, with particular thanks to M. Billing, D. Sagan, D. Hartill, D. Rice, and Y. Li, for useful discussions. This work has been supported by the National Science Foundation.

[1] L. E. Sakazaki, R. M. Littauer, R. H. Siemann, and R. M. Talman, IEEE Trans. Nucl. Sci. **32**, 2353 (1985); L. E. Sakazaki, Ph.D. thesis, Cornell University, 1985.
[2] M. G. Billing, M. Giannella, R. M. Littauer, and G. R. Rouse, in *Proceedings of the 1989 IEEE Particle Accelerator Conference* (IEEE, New York, 1989), p. 1163.
[3] R. Littauer, Cornell Laboratory of Nuclear Studies Report No. CLNS 88/847, 1988 (unpublished).
[4] D. L. Hartill, T. Holmquist, J. T. Rogers, and D. C. Sagan, Cornell Laboratory of Nuclear Studies Report No. CBN 95-3, 1995 (unpublished).
[5] D. Sagan and J. J. Welch, Cornell Laboratory of Nuclear Studies Report No. CBN 92-1, 1992 (unpublished).
[6] T. Holmquist, M.S. thesis, Cornell University, 1996.
[7] J. T. Rogers, in *Proceedings of the 1995 Particle Accelerator Conference, Dallas* (IEEE, New York, 1995), p. 3052.
[8] O. Grobner *et al.,* J. Vac. Sci. Technol. A **7**, 223 (1989).
[9] M. A. Furman and G. R. Lambertson, in *Proceedings of the 1996 European Particle Accelerator Conference, Barcelona* (Institute of Physics, Bristol, U.K., 1996), p. 1087; F. Zimmermann, CERN LHC Project Report No. 95, 1997 (unpublished).
[10] A. Chao, *Physics of Collective Instabilities in High Energy Accelerators* (Wiley, New York, 1993).
[11] K. Ohmi, Phys. Rev. Lett. **75**, 1526 (1995); S. Heifets, Stanford Linear Accelerator Center Report No. SLAC-AP-95-101, 1995 (unpublished).
[12] M. Izawa, Y. Sato, and T. Toyomasu, Phys. Rev. Lett. **74**, 5044 (1995).
[13] Z. Y. Guo *et al.,* in Proceedings of the 1997 Particle Accelerator Conference, Vancouver (to be published).